

Ultrahigh-sensitivity sensors based on thin-film coated long period gratings with reduced diameter, in transition mode and near the dispersion turning point

Ignacio Del Villar

Electrical and Electronic Engineering Department, Public University of Navarra, 31006 Pamplona, Spain
ignacio.delvillar@unavarra.es

Abstract: The mode transition and the dispersion turning point have been explored for optimization of thin-film coated long period fiber gratings during the last years. In this work an additional parameter, the cladding diameter, is combined with the other two phenomena for improving the sensitivity to the surrounding medium refractive index. The numerical data obtained were calculated with a method based on the exact calculation of core and cladding modes and the utilization of coupled mode theory. A sensitivity 143×10^3 nm/RIU is obtained, the highest reported so far with long period fiber gratings.

©2015 Optical Society of America

OCIS codes: (060.2370) Fiber optics sensors; (060.3735) Fiber Bragg gratings; (240.0310) Thin films.

References and links

1. B. Lee, "Review of the present status of optical fibre sensors," *Opt. Fiber Technol.* **9**(2), 57–79 (2003).
2. C. R. Zamarreño, J. M. Corres, J. Goicoechea, I. Del Villar, I. R. Matias, and F. J. Arregui, "Fibre Optic Nanosensors," in *Optochemical Nanosensors*, A. Cusano, F. J. Arregui, M. Giordano, and A. Cutolo, (Taylor and Francis, 2012).
3. W. G. J. H. M. van Sark, "Deposition and processing of thin films" in *Handbook of Thin Films*, H. S. Nalwa, (Elsevier, 2002).
4. N. D. Rees, S. W. James, R. P. Tatam, and G. J. Ashwell, "Optical fiber long-period gratings with Langmuir-Blodgett thin-film overlays," *Opt. Lett.* **27**(9), 686–688 (2002).
5. I. Del Villar, M. Achaerandio, I. R. Matías, and F. J. Arregui, "Deposition of an Overlay with Electrostatic Self-Assembly Method in Long Period Fiber Gratings," *Opt. Lett.* **30**(7), 720–722 (2005).
6. I. Del Villar, I. R. Matias, F. J. Arregui, and M. Achaerandio, "Nanodeposition of Materials with complex refractive index in Long Period Fiber Gratings," *J. Lightwave Technol.* **23**(12), 4192–4199 (2005).
7. I. Del Villar, I. R. Matias, and F. J. Arregui, "Influence on cladding mode distribution of overlay deposition on long-period fiber gratings," *J. Opt. Soc. Am. A* **23**(3), 651–658 (2006).
8. A. Cusano, A. Iadicicco, P. Pilla, L. Contessa, S. Campopiano, A. Cutolo, and M. Giordano, "Cladding mode reorganization in high-refractive-index-coated long-period gratings: effects on the refractive-index sensitivity," *Opt. Lett.* **30**(19), 2536–2538 (2005).
9. I. Del Villar, I. Matías, F. Arregui, and P. Lalanne, "Optimization of sensitivity in Long Period Fiber Gratings with overlay deposition," *Opt. Express* **13**(1), 56–69 (2005).
10. A. Cusano, A. Iadicicco, P. Pilla, L. Contessa, S. Campopiano, A. Cutolo, and M. Giordano, "Mode transition in high refractive index coated long period gratings," *Opt. Express* **14**(1), 19–34 (2006).
11. P. Pilla, A. Iadicicco, L. Contessa, S. Campopiano, A. Cutolo, M. Giordano, G. Guerra, and A. Cusano, "Optical chemo-sensor based on long-period gratings coated with δ form syndiotactic polystyrene," *IEEE Photon. Technol. Lett.* **17**(8), 1713–1715 (2005).
12. J. M. Corres, I. del Villar, I. R. Matias, and F. J. Arregui, "Fiber-optic pH sensors in Long-Period Gratings using Electrostatic Self-Assembly," *Opt. Lett.* **32**(1), 29–31 (2007).
13. F. Chiavaioli, P. Biswas, C. Trono, S. Bandyopadhyay, A. Giannetti, S. Tombelli, N. Basumallick, K. Dasgupta, and F. Baldini, "Towards sensitive label-free immunosensing by means of turn-around point long period fiber gratings," *Biosens. Bioelectron.* **60**, 305–310 (2014).
14. X. Shu, L. Zhang, and I. Bennion, "Sensitivity Characteristics of Long-Period Fiber Grating," *J. Lightwave Technol.* **20**(2), 255–266 (2002).
15. Z. Wang, J. Heflin, R. Stolen, and S. Ramachandran, "Analysis of optical response of long period fiber gratings to nm-thick thin-film coating," *Opt. Express* **13**(8), 2808–2813 (2005).

16. C. S. Cheung, S. M. Topliss, S. W. James, and R. P. Tatam, "Response of fiber-optic long-period gratings operating near the phase-matching turning point to the deposition of nanostructured coatings," *J. Opt. Soc. Am. B* **25**(6), 897–902 (2008).
17. P. Pilla, C. Trono, F. Baldini, F. Chiavaioli, M. Giordano, and A. Cusano, "Giant sensitivity of long period gratings in transition mode near the dispersion turning point: an integrated design approach," *Opt. Lett.* **37**(19), 4152–4154 (2012).
18. M. Śmietana, M. Koba, P. Mikulic, and W. J. Bock, "Measurements of reactive ion etching process effect using long-period fiber gratings," *Opt. Express* **22**(5), 5988–5994 (2014).
19. T. Erdogan, "Fiber Grating Spectra," *J. Lightwave Technol.* **15**(8), 1277–1294 (1997).
20. E. Anemogiannis, E. N. Glytsis, and T. K. Gaylord, "Transmission characteristics of long- period fiber gratings having arbitrary azimuthal/radial refractive index variation," *J. Lightwave Technol.* **21**(1), 218–227 (2003).
21. T. Erdogan, "Cladding-mode resonances in short- and long-period fiber gratings filters," *J. Opt. Soc. Am. A* **14**(8), 1760–1773 (1997).
22. G. P. Agrawal, *Nonlinear fiber optics 3rd ed.* (Academic Press: New York, 2001), p. 8.
23. A. B. Socorro, I. Del Villar, J. M. Corres, F. J. Arregui, and I. R. Matias, "Spectral width reduction in lossy mode resonance-based sensors by means of tapered optical fibre structures," *Sens. Actuators B Chem.* **200**, 53–60 (2014).
24. I. Del Villar, I. R. Matias, and F. J. Arregui, "Long-period fiber gratings with overlay of variable refractive index," *IEEE Photon. Technol. Lett.* **17**(9), 1893–1895 (2005).

1. Introduction

The deposition of thin-films on optical fibre substrates has permitted, during the last decade, to widen the traditional domains of application of optical fibre sensors (e.g. strain and temperature [1]) to other research fields [2]. This has been possible thanks to the development of techniques [3], that allow coating the optical fibre with materials, which properties change as a function of a biological or chemical species.

In the domain of long period fibre gratings (LPFGs), the utilization of thin-films has permitted both to increase the number of applications and to optimize the sensitivity of the devices. In the first work with thin-film coated LPFGs it was observed that the attenuation bands in the optical spectrum experimented important wavelength shifts as a function of the thin-film thickness [4]. The technique used for the thin-film deposition was Langmuir Blodgett and there was a region where the attenuation bands faded. In a later work based on Layer-by-Layer (LbL) self-assembly [5], again the same fading region was obtained as a function of thickness. However, in this work it was proved, with a theoretical model based on coupled mode theory and the calculation of LP modes in a cylindrical multilayer waveguide, that in the fading region the Bragg condition was still satisfied. The fading was caused by inherent losses of the thin-film [6] and the reduction of the coupling coefficient of cladding modes in this region, which can be also analyzed with a vectorial model based on hybrid modes [7]. Also in the year 2005, the possibility of using dip-coating technique permitted to reduce the inherent losses of the material deposited sufficiently to avoid the fading region [8], and to obtain a highest sensitivity for an adequate selection of thin-film thickness and refractive index, and surrounding medium refractive index [9]. Since this high sensitivity is obtained thanks to a transition to guidance of a cladding mode in the overlay [5], the phenomenon started to be called as mode transition (MT) [10]. This permitted to develop interesting applications such as chemical sensors, humidity sensors or biosensors [11–13].

Another important phenomenon in LPFGs is the dispersion turning point (DTP) [14], which also permits to increase the sensitivity of these devices.

The combination of DTP with a thin-film coated LPFG was first explored in [15]. However, it was not possible to combine the DTP with the MT phenomenon due to the low thin-film thickness. This was achieved in [16].

Recently, the optimization of the combination of both phenomena has permitted to achieve sensitivities approaching 10000 nm/RIU [17], and in other works the reduction of the diameter of LPFGs has led to a sensitivity improvement [13,18], which indicates that the sensitivity limit has not been reached yet.

In this work the DTP, the MT and the reduction of the diameter of LPFGs is analyzed theoretically towards obtaining the highest sensitivity reported with this type of optical fiber devices.

The remainder of this work is organized as follows. In section 2 the numerical method used in sections 3 and 4 is described. After that, in section 3 LPFGs near the DTP are analyzed as a function of the diameter. In section 4 an additional parameter is introduced: the presence of a thin film. Finally, some conclusions are included in section 5.

2. Theory

In this work the vectorial method described in [7] is used. It is basically an expansion of the coupled mode method of Erdogan for a multilayer structure [19] and follows the same steps indicated in [9], where the LP mode approximation is used. The only difference is the utilization of hybrid modes. In [7] it was explained that, for specific cases, the LP mode approximation is not valid with thin-film coated LPFGs. Consequently, a method based on the exact solutions of the modes has been used.

When analyzing LPFG structures, the application of the modified first-order Bragg condition permits to obtain the resonance wavelengths with errors lower than 0.1% [20]:

$$\beta_{11}(\lambda) + s_0 \zeta_{11,11}(\lambda) - (\beta_{1j}(\lambda) + s_0 \zeta_{1j,1j}(\lambda)) = \frac{2\pi N}{\Lambda} \quad (1)$$

where β_{11} and β_{1j} are the propagation constants of the core and the j cladding modes respectively, Λ is the period of the grating, $\zeta_{11,11}$ and $\zeta_{1j,1j}$ are the self-coupling coefficients of the core and the j cladding modes, s_0 is the coefficient of the first Fourier component of the grating and N is the diffraction order.

However, the power transmitted versus wavelength offers more information than expression (1) and it will be used for some of the results of sections 3 and 4. To this purpose, couple-mode theory is necessary.

The generalized couple-mode equations describing an LPFG can be expressed as [19,21]:

$$\frac{dF_{1k}(z)}{dz} = -j \sum_{j=1}^M K_{1j,1k} F_{1j}(z) \exp(-j(\beta_{1j} - \beta_{1k})z) \quad \text{for } k = 1, 2, \dots, M \quad (2)$$

which can be expressed in a matrix form in the following way:

$$\begin{pmatrix} \dot{F}_{11}(z) \\ \dot{F}_{12}(z) \\ \vdots \\ \dot{F}_{1N}(z) \end{pmatrix} = \begin{pmatrix} Q_{11} & V_{12,11} & \cdots & V_{1N,11} \\ V_{11,12} & Q_{12} & \cdots & V_{1N,12} \\ \vdots & \vdots & \ddots & \vdots \\ V_{11,1N} & V_{12,1N} & \cdots & Q_{1N} \end{pmatrix} \begin{pmatrix} F_{11}(z) \\ F_{12}(z) \\ \vdots \\ F_{1N}(z) \end{pmatrix} \quad (3)$$

where F_{1j} is the normalized amplitude of the j mode, and the Differential Equation (DE) matrix elements are defined as:

$$Q_{1j} = -j\sigma(z)s_0\zeta_{1j,1j} \quad (4)$$

$$V_{1j,1k} = -j\sigma(z)\frac{s_1}{2}\zeta_{1j,1k}\exp\left[-jz\left(\beta_{1j} - \beta_{1k} \pm \frac{2\pi}{\Lambda}\right)\right] \quad (5)$$

where s_0 and s_1 are the coefficients of the first two Fourier components of the grating function. The \pm sign in the exponential function depends on the sign of the difference between the propagation constants of the modes, which permits the coupling between each pair of them. If $\beta_{1j} > \beta_{1k}$, the minus sign is selected; otherwise the plus sign is chosen.

The transmission can be found by assuming that only one mode is incident ($F_{11}(0) = 1$ and $F_{12}(0) = \dots = F_{1N}(0) = 0$) and solving the differential equation. The transmitted power at the end of the LPFG can be expressed as:

$$\frac{F_{11}(L)^2}{F_{11}(0)^2} \quad (6)$$

3. Optimization of sensitivity in uncoated long-period fiber gratings

A commercial LPFG is selected for the analysis performed in this section. A modulation of the core refractive index is induced in a SMF28 single mode fiber.

The parameters of the LPFGs analyzed are: core diameter 8.3 μm , cladding diameter 125 μm , core diameter + 0,36% the cladding diameter, cladding refractive index that of silica [22]. The surrounding medium refractive index (SRI) is 1.33 (water). The modulation of the grating is considered sinusoidal, and the amplitude of the modulation is 1.75×10^{-4} . The notation used for the modes is: $\text{HE}_{1,1}$ for the core mode; $\text{HE}_{1,2}$ for the first $\text{HE}_{1,j}$ cladding mode, $\text{HE}_{1,4}$ for the second $\text{HE}_{1,j}$ cladding mode, and so on; $\text{EH}_{1,3}$ for the first $\text{EH}_{1,j}$ cladding mode, $\text{EH}_{1,5}$ for the second $\text{EH}_{1,j}$ cladding mode, and so on. In order to compare with other works where LP approximation is used, the equivalent of $\text{HE}_{1,2}$ is $\text{LP}_{0,2}$, the equivalent of $\text{HE}_{1,4}$ is $\text{LP}_{0,3}$, the equivalent of $\text{HE}_{1,6}$ is $\text{LP}_{0,4}$, and so on.

In Fig. 1(a) expression (1) is used to calculate the resonance wavelength versus grating period for an LPFG of diameter 125 μm . $\text{HE}_{1,20}$ is in the dispersion turning point approximately in the wavelength range 1400-1650 nm. By obtaining plots of the resonance wavelength versus the grating period for different cladding diameters it has been checked that as the diameter of the optical fiber is reduced, the lines satisfying the Bragg condition shift to lower grating period values. As an example, results corresponding to an LPFG of diameter 113.03 μm (11.97 μm less than the LPFG of 125 μm), are presented in Fig. 1(b). This value has been selected because for this diameter $\text{HE}_{1,18}$ takes the place of the $\text{HE}_{1,20}$ mode, which is the mode in the dispersion turning point in Fig. 1(a).

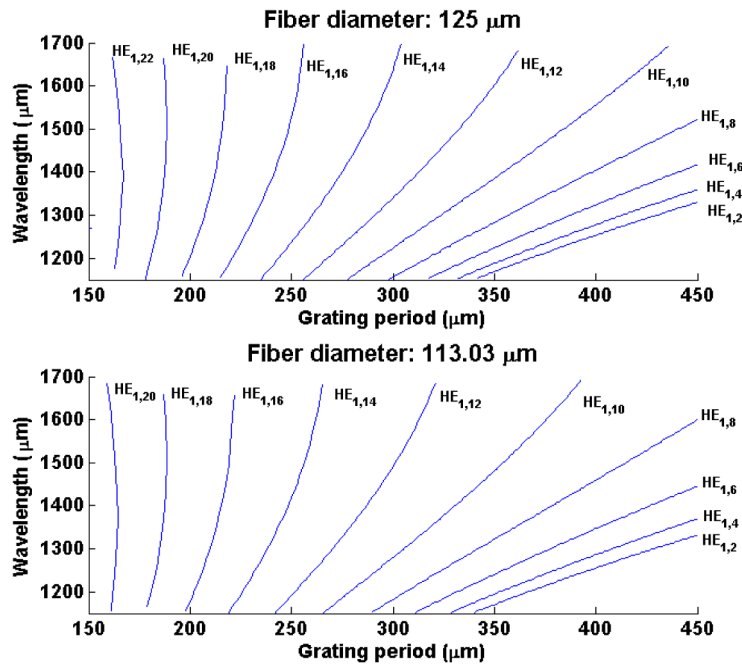


Fig. 1. Calculated variation of mode resonance wavelength with LPFG period for a) cladding diameter 125 μm ; b) cladding diameter 113.03 μm . SRI = 1.33. The LPFGs are uncoated.

The periodicity of the phenomenon is repeated up to the lowest order mode. In Fig. 2(a), the results correspond to an LPFG with diameter 41.21 μm ($125 \mu\text{m} - 7 \times 11.97 \mu\text{m}$), and the line for $\text{HE}_{1,6}$ mode is in the range of period 150-200 μm . In Fig. 2(b), the results correspond

to an LPFG with diameter $29.24\ \mu\text{m}$ ($125\ \mu\text{m} - 8 \times 11.97\ \mu\text{m}$), and the line for $\text{HE}_{1,4}$ mode is in the range of period $150\text{-}200\ \mu\text{m}$. Finally, the same is true in Fig. 2(c) with the lowest order cladding mode ($\text{HE}_{1,2}$ mode) for an LPFG with diameter $17.27\ \mu\text{m}$ ($125\ \mu\text{m} - 9 \times 11.97\ \mu\text{m}$).

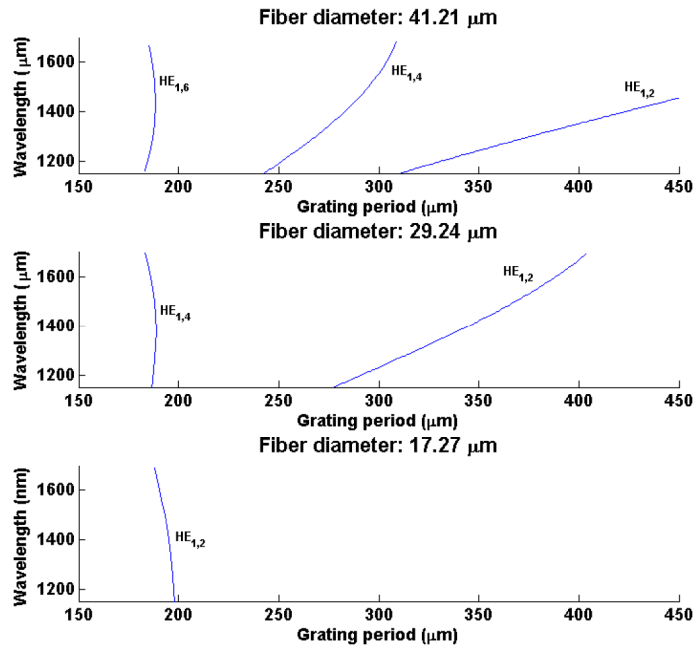


Fig. 2. Calculated variation of mode resonance wavelength with LPFG period for a) cladding diameter $41.31\ \mu\text{m}$; b) cladding diameter $29.24\ \mu\text{m}$; c) cladding diameter $17.27\ \mu\text{m}$. SRI = 1.33. The LPFGs are uncoated.

Now a period of $188\ \mu\text{m}$ is used for analyzing the sensitivity of the previous LPFGs. This value was selected because for the LPFGs analyzed permits to obtain two attenuation bands situated close to the dispersion turning point (see Fig. 3 and Fig. 4). The numerical data were obtained by application of the coupled mode equations (expression 2). If a grating length of $40\ \text{mm}$ is used for all LPFGs, there is a progressive reduction of the attenuation band depth (see Fig. 3).

Consequently, a linear reduction as a function of the grating length was chosen, which permitted to avoid this issue down to a diameter $41.21\ \mu\text{m}$ (Fig. 2(a)). For a diameter $41.21\ \mu\text{m}$ a grating length of $22.5\ \text{mm}$ was chosen and all other lengths were linearly interpolated with the $40\ \text{mm}$ length of LPFG of diameter $125\ \mu\text{m}$. This permitted to obtain in the upper four subplots of Fig. 4 attenuation bands with depths higher than $20\ \text{dB}$. However, this was not the case for the lower two subplots in Fig. 4. The explanation is that as the diameter approaches that of the core, the evolution in the reduction in the depth of the attenuation bands cannot be compensated linearly with a reduction of the grating length. However, attenuation bands obtained are still adequate for the evaluation of the sensitivity.

Henceforward the sensitivity will be expressed as the increase in the spectral distance between the two attenuation bands in the optical spectrum divided by the variation of the SRI [18].

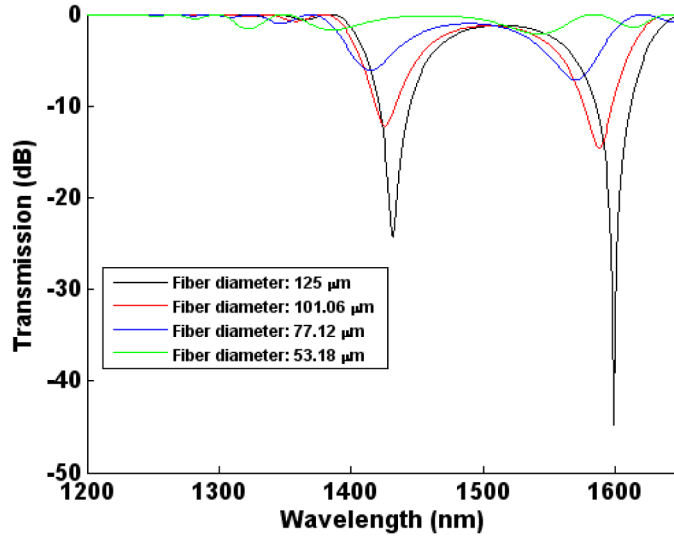


Fig. 3. Transmission spectra for uncoated LPFG of cladding diameter 125 μm , 101.06 μm , 77.12 μm and 53.18 μm . Grating length 40 mm. SRI 1.33. The attenuation bands fade progressively as the LPFG diameter is reduced.

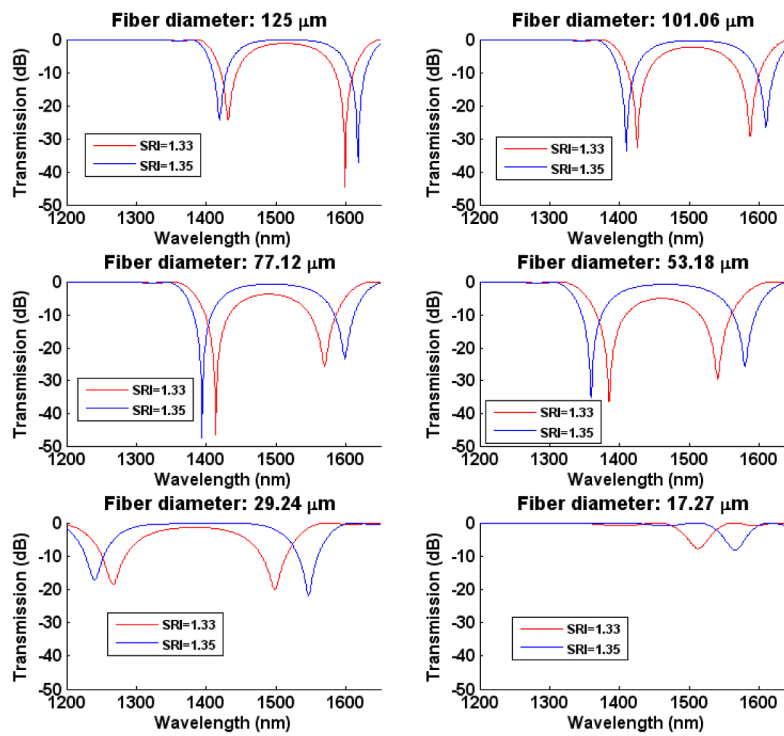


Fig. 4. Transmission spectra for 6 LPFGs as a function of the cladding diameter. The grating period is 188 μm . SRI values: 1.33 and 1.35.

In Fig. 4 the sensitivity for the 125 μm LPFG is 1600 nm/RIU, the sensitivity for the 29.24 μm LPFG is 3750 nm/RIU and the sensitivity for the 17.27 μm LPFG is 2650 nm/RIU. It is important to indicate that, even though the sensitivity for the 17.27 μm LPFG is lower than the sensitivity of the 29.24 μm LPFG, it is because in the transmission spectrum there is only one

attenuation band visible (for comparison the sensitivity of the right band in the transmission spectrum of the 29.24 μm LPFG is 2400 nm/RIU). This agrees with Fig. 2(c), where for the LPFG of diameter 17.27 μm there is no dispersion turning point. This issue could be solved by increasing the diameter of 17.27 μm in this last LPFG. The line of Fig. 2(c) would shift to a higher grating period and the dispersion turning point would be obtained. This idea will be applied with thin-film coated LPFGs, where this phenomenon is more dramatic, in the next section.

4. Optimization of sensitivity in thin-film coated long-period fiber gratings

The parameters of the LPFGs analyzed in this section will be the same as those used in section 3. The main difference will be now the inclusion of a thin-film on the cladding of the LPFG. The refractive index of the thin-film will be 1.55, which is a typical value of polymer coatings [17, 23].

First the variation of the effective index of cladding modes will be analyzed as a function of the coating thickness for an LPFG of diameter 125 μm . The mode transition is a well-known phenomenon [5–10]. Consequently, focus will only be centred on the derivative of the effective index of cladding modes versus coating thickness. The wavelength used for the analysis is 1450 nm. In Fig. 5, the maximum derivative for the effective index of $\text{HE}_{1,20}$ is 313 nm , which will be the value used henceforward.

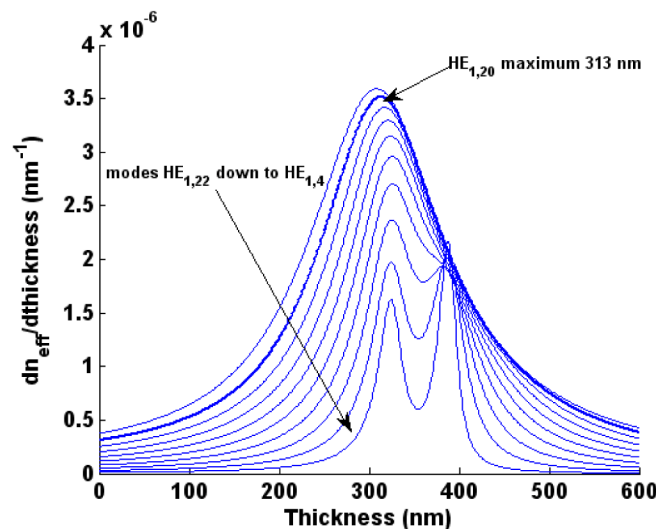


Fig. 5. $dn_{\text{eff}}/d\text{thickness}$ as a function of thickness for an LPFG with cladding diameter 125 μm .

In Fig. 6(a), the resonance wavelength versus grating period can be observed for a thin-film coated LPFG of diameter 125 μm . It is important to note that, unlike Fig. 1, the DTP for $\text{HE}_{1,20}$ is shifted to lower wavelengths. However, the thin-film thickness has been optimized for a highest sensitivity at 1450 nm. Consequently, in order to set the dispersion turning point centre at this wavelength it is necessary to reduce the LPFG diameter to 124 μm (see Fig. 6(b)).

In Fig. 7, results for LPFGs with diameters 57 μm , 46 μm and 34.8 μm are presented. They show the DTP at 1450 nm for modes $\text{HE}_{1,8}$, $\text{HE}_{1,6}$ and $\text{HE}_{1,4}$ respectively. $\text{HE}_{1,2}$ is not considered because this mode is guided in the thin-film in the MT.

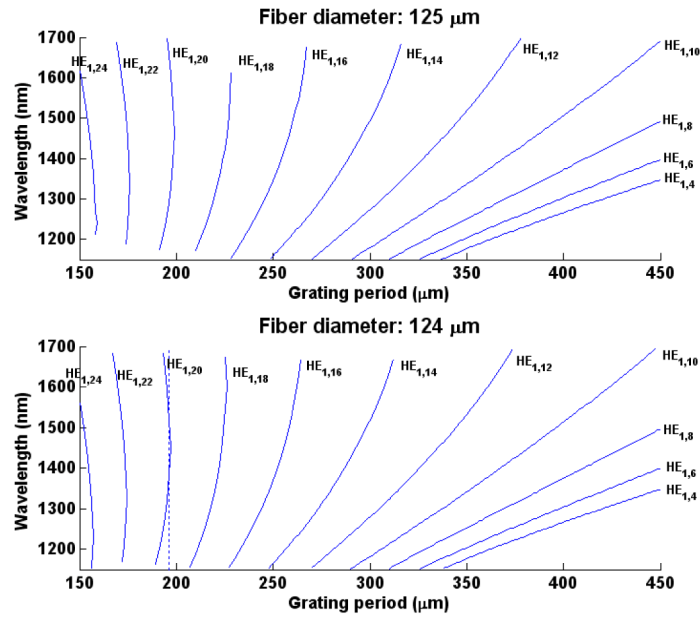


Fig. 6. Calculated variation of mode resonance wavelength with LPFG period for a) cladding diameter 125 μm; b) cladding diameter 124 μm. The LPFG is covered with a 313 nm thin-film. SRI = 1.33.

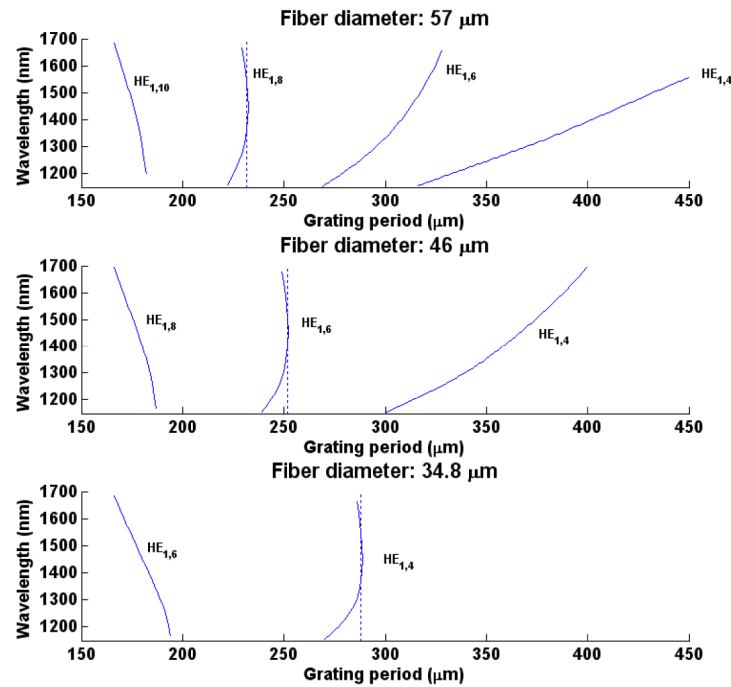


Fig. 7. Calculated variation of mode resonance wavelength with LPFG period for a) cladding diameter 57 μm; b) cladding diameter 46 μm; c) cladding diameter 34.8 μm. The LPFG is covered with a 313 nm thin-film. SRI = 1.33.

In Fig. 6 and Fig. 7 an additional line with the period selected for sensitivity analysis is added for LPFGs with diameter 124 μm , 57 μm , 46 μm and 34.8 μm . The grating periods for these LPFGs are 196, 231.6, 251.7 and 288.1 μm respectively. With these grating periods it is possible to obtain two attenuation bands in Fig. 8 with the same separation from each other as in Fig. 4 for the sake of comparison. The increase in the period for lower cladding modes confirms the idea proposed in section 2 for the LPFG of diameter 17.27 μm , where it was suggested to increase the grating period to fit the dispersion turning point. In Fig. 8 an additional plot for a refractive index 1.331 is added for obtaining the sensitivity, which is 16×10^3 nm/RIU, 33×10^3 nm/RIU, 47×10^3 nm/RIU and 79×10^3 nm/RIU, for LPFGs with diameter 124 μm , 57 μm , 46 μm and 34.8 μm respectively.

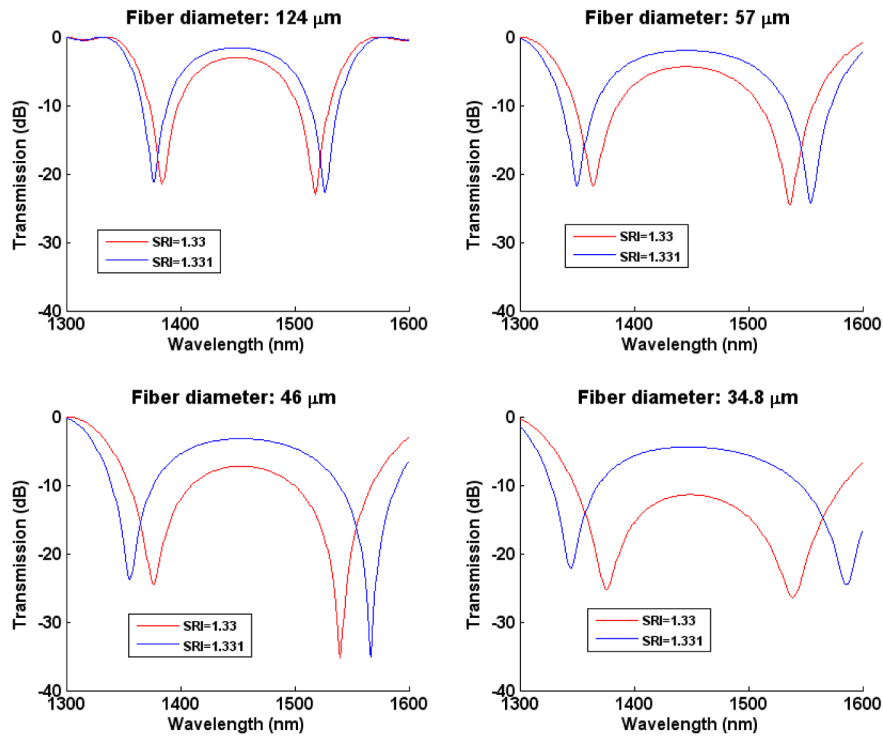


Fig. 8. Transmission spectra for 4 LPFGs for different combinations of cladding diameter and grating length. SRI values: 1.33 and 1.331.

Finally, in order to exploit the maximum sensitivity of thin-film coated LPFGs, if the period of the LPFG of diameter 34.8 μm is increased to 288.5 μm for approaching the DTP, a sensitivity 143×10^3 nm/RIU is obtained in the range 1.33 to 1.331 (see Fig. 9), the highest reported so far for an LPFG. This should permit to improve the resolution of LPFG based chemical and biological sensors. Moreover, according to [24] the sensitivity of LPFGs could even be further improved by deposition of coatings with very high refractive index.

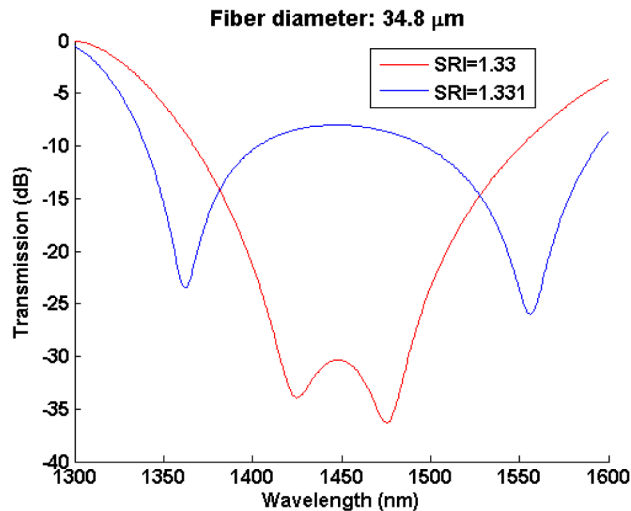


Fig. 9. Transmission spectra for an LPFG with 34.8 μm and grating period is 288.5 μm. SRI values: 1.33 and 1.331.

5. Conclusion

In this work it has been analyzed with a numerical method based on coupled mode theory and a vectorial calculation of the cladding and core modes the optimization of an LPFG based on three factors: the transition of modes, the dispersion turning point and the reduction of the cladding diameter.

Both coated and uncoated structures have been analyzed. In all cases the reduction of the cladding diameter leads to an improvement in sensitivity. However, this is more dramatic in the case of coated LPFGs working at the mode transition region.

A record sensitivity of 143×10^3 nm/RIU has been obtained, the highest sensitivity reported so far with LPFGs. This indicates the ability of LPFGs to compete with other devices such as surface plasmon resonance (SPR) sensors. Moreover, the presented results should permit to improve the resolution of LPFG based chemical and biological sensors.

Acknowledgements

This work was supported in part by the Spanish Ministry of Education and Science-FEDER TEC2013-43679-R.